National Oceanography Centre, Southampton

Internal Document No. 4

Validation of the VECTIS steady-state solver

B I Moat & M J Yelland

2006

National Oceanography Centre, Southampton
University of Southampton, Waterfront Campus
European Way
Southampton
Hants SO14 3ZH
UK

Author contact details
Tel: +44 (0)23 8059 7739
Fax: +44 (0)23 8059 6404
Email: ben.moat@noc.soton.ac.uk

DOCUMENT DATA SHEET

AUTHOR
MOAT, B I & YELLAND, M J

PUBLICATION DATE 2006

TITLE
Validation of the VECTIS steady-state solver.

REFERENCE
Southampton, UK: National Oceanography Centre, Southampton, 15pp.
(National Oceanography Centre Southampton Internal Document, No. 4) (Unpublished manuscript)

ABSTRACT

Wind speed measurements are obtained from anemometers located on research ships. Even though the anemometers are usually positioned in well-exposed locations the presence of the ship's hull and superstructure distorts the airflow to the anemometer and biases the wind speed measurements. Previous studies have shown biases of up to 10 % for bow-on flows, and that the biases generally increase for other wind directions. Corrections for the effects of the flow distortion are vital, as these data are used for satellite validation and in climate related studies. Therefore, the computational fluid dynamics (CFD) package VECTIS is used to numerically simulate the airflow over ships and derive corrections for this effect.

A VECTIS simulation of one ship at one wind direction currently takes approximately one month to perform on a typical UNIX workstation. Therefore, it would be impractical to study the airflow over a large number of research ships and/or a large number of wind directions. A faster method (the "steady-state solver") for VECTIS simulations has been available for some time, but requires significant increases in computational speed and memory which have only recently become widely available. This report presents a comparison of VECTIS simulations using the steady-state solver with both previous VECTIS studies and in situ wind speed measurements.

Use of the steady-state solver requires a higher mesh density but also cuts model convergence times from weeks to days, allowing fine-resolution models to be run without impractical time-constraints. The results of this study show that in regions where the flow distortion is high, the increased mesh density results in significant improvement in the comparison between modelled and in-situ wind speeds.

KEYWORDS
AIRFLOW DISTORTION, COMPUTATIONAL FLUID DYNAMICS, CFD, RRS *DISCOVERY*, WIND SPEED MEASUREMENT,

ISSUING ORGANISATION
National Oceanography Centre, Southampton
University of Southampton, Waterfront Campus
European Way
Southampton SO14 3ZH
UK

VALIDATION OF THE VECTIS STEADY-STATE SOLVER

VALIDATION OF THE VECTIS STEADY-STATE SOLVER

B. I. Moat an M. J. Yelland

August 2006

1. Introduction

The computational fluid dynamics (CFD) code VECTIS has been used since 1994 to numerically simulate the airflow over many research ships and derive corrections for the effects of flow distortion (Yelland et al., 1998, 2002). Details of other methods used to model the airflow over ships are given in Moat et al. (2005).

Until recently, VECTIS has taken about four weeks of computer time to simulate the airflow over one ship at one relative wind direction which has made it impractical to model many ships or many wind directions. However, with the continual increase in computing power and memory size it is now possible to use the dedicated steady-state solver within VECTIS, rather than the time-marching solver previously used. The steady-state solver computes simulations using a finer mesh resolution than that used in previous studies, which generally increases the model accuracy, in a shorter time. This report will discuss the reduction in model convergence times for VECTIS simulations using the steady-state solver and check the accuracy of the simulation by comparison to previous results.

A brief description of VECTIS is contained in Section 2. Yelland et al. (2002) (hereafter Y2002) simulated the airflow over a number of ships using VECTIS and validated the model results by comparing those for the *RRS Discovery* to in situ wind speed measurements made from the same ship. In the present study the airflow over the RRS *Discovery* is simulated using the steady-state solver and the results are compared to those of Y2002. The findings of this comparison are discussed in Section 3.

2. CFD model description

The commercially available CFD package VECTIS (Ricardo, 2005) is used to calculate the three-dimensional, compressible, steady-state solutions to the Reynolds-Averaged Navier-Stokes continuity and energy equations. The simulations are based on a non-uniform Cartesian mesh. The code uses the $k \sim \varepsilon$ turbulence closure model of Launder and Spalding (1974) with standard coefficients. It should be noted that the

models are used to investigate the mean flow properties (mean wind speed and vertical displacement of the flow) only. The turbulent properties of the flow are not examined. Further details on the application and operation of VECTIS are given in Y2002 and Moat (2003), and will only be summarized here.

The accuracy of CFD codes are significantly dependant upon the computational mesh size and type, numerical schemes and the turbulence closure scheme (Cowen et al., 1997). In particular, the smaller the computational mesh the more accurate the solution, e.g. in an ideal world simulations would be solved using an incredibly fine mesh where the smallest cells are smaller than the smallest feature of the flow. Such simulations are currently impractical for flows over a ship, as the number of cells required would be of the order 10^{29} (Ferziger, 2000) and would take decades to run at the present state of computing power. Therefore compromises have to be made in defining the mesh resolution to achieve realistic convergence times to a given accuracy. To improve efficiency the number of cells within the VECTIS simulations are increased in specific areas of interest, such as the regions where anemometers are located, and reduced elsewhere. The number of cells employed by VECTIS is limited by the amount of memory in the machine used to compute the solution. All VECTIS airflow simulations require 1 Mb of memory per 1000 cells regardless of the solver. Convergence times for VECTIS simulations vary with both the number of cells specified and the solver method employed. This is discussed below.

To date, VECTIS simulations of flow over ships have employed a time-marching (TM) method to calculate a steady-state solution, i.e. all equations were solved to a specified tolerance at each time step. This is a robust method that minimises the amount of memory required to calculate a steady-state solution, but it can take a long time to complete a simulation, e.g. recent simulations based on 500,000 cells take up to 3 weeks using a Linux workstation with a 2.4 GHz Opteron processor. Increasing the cell resolution to that used by the steady-state solver used in the current study (one million cells) would probably extend the run times to about six weeks, or more, using the Linux workstation specified above.

With recent increases in computational speed and memory it is now possible to employ the steady-state solver (hereafter SSS). The SSS directly solves the same equations as the TM method, but to be numerically stable it requires that the aspect ratio of the sides of each cell be 1.5, i.e. for a cell of length 0.5 m the other sides are

restricted to a maximum size of 0.75 m. Therefore, a much greater number of cells are required to solve the flow field. Typically, about one million cells (1Gb of memory) are required for a bow-on flow over a research ship, i.e. seven times the number of cells (150,000) used in the Y2002 study. This increases to about 3Gb for airflows at 30° off the bow (Moat et al., 2006), as the number of cells increases to accommodate the larger computational domain used. These memory requirements mean that the SSS can only be run on high-end PCs and workstations. The SSS simulation with 1,000,000 cells converged to a steady-state in 5 days using a Linux workstation with a 2.4 GHz Opteron processor. This compares to 3 weeks for the original Y2002 simulation (performed on a SGI Indigo^2 workstation using 150,000 cells). If the Y2002 simulation of 150,000 cells was reproduced on the Linux box specified above the model would probably converge in a similar time to the 1 million SSS solution, i.e. 5 days. In other words, it is estimated that use of the SSS reduces the convergence time by a factor of 7. Table 1 summarises VECTIS the run times using the two different methods.

A major benefit of the SSS method is the ability to specify a higher cell resolution over most of the ship, rather than just one or two small areas, without extending run times beyond about 1 week. This allows a greater number of instrument sites to be studied in more much detail than was previously feasible. Figure 1 shows the cell resolutions used in the Y2002 and the SSS studies. It can be seen that a) the region of high mesh density was restricted to the regions close to the instrument sites in the 2002 model, but extends over the whole forward half of the ship in the current study, and b) the areas of high mesh density have larger cell sizes in the Y2002 model than in the SSS model. The cell sizes in the regions where the Y2002 anemometers were located are given in Table 2.

In this study, the Y2002 simulation of a bow-on flow over the RRS *Discovery* was repeated using the SSS instead of the original time-marching solver. The same boundary conditions were applied to both simulations, i.e. a semi-logarithmic wind speed profile with a 14 ms^{-1} wind speed specified at a height of 10 m. Due to the increased number of cells required by the SSS the same mesh could not be used. With the exception of a modification to relocate an incorrectly positioned lifting gantry on the forecastle of the ship, the geometry was the same in both simulations (Figure 1). It

should be noted that the gantry was located too far from the anemometer locations to affect the airflow to them.

3. Comparison of the CFD and in situ wind speed results

3.1 Method

The Y2002 in situ wind speed data were collected from a number of anemometers located at various positions on the RRS *Discovery* (Figure 1). A Solent sonic anemometer, a Windmaster sonic anemometer and a Young propeller vane were all located on the foremast platform (Figure 2). A second Solent sonic was located on the main mast above the bridge. Two temporary masts were located above the lifeboat deck and the bridge (Figure 1). Each mast was instrumented with 5 Vector cup anemometers. Details of the instrument heights are given in Table 3. Both Vector cup anemometer masts were intentionally located in regions of severe flow distortion for the purpose of CFD code validation.

A direct comparison of the CFD model wind speeds with the in situ wind speed data was not possible since there was no in situ measurement of the undistorted, or freestream, flow. Instead, for each anemometer site a relative difference was obtained by dividing the wind speed measured by each anemometer with that from a well-exposed reference anemometer. In this case the Solent sonic located on the foremast platform was used as the reference. A comparison of the SSS CFD results with the previous in situ and TM CFD results of Y2002 for the well-exposed anemometers for a flow directly over the bow are examined in Section 3.2. Similarly a comparison of the in situ and model results for the badly exposed Vector anemometers is examined in Section 3.3. Section 3.4 discusses the absolute wind speed biases and the vertical displacement of the flow.

3.2 Relative wind speed difference at the well-exposed anemometer sites

Figure 3 compares the Y2002 in situ and CFD model estimates of the relative wind speed differences for the foremast and main mast anemometers with the SSS results. Table 3 contains the differences between the CFD model estimates and the in situ wind speed data. For the foremast sites, both models underestimate the in situ wind speed data by between 2 % to 3 %. The SSS model relative wind speed differences agreed with the Y2002 model results to within 0.2 %. For the main mast anemometer site both models over-estimate the relative difference by 2.5 % compared to the in situ

data, with the SSS model agreeing exactly with the Y2002 model. This shows that a) the Y2002 solution, based on a coarser mesh, was independent of the cell size (Table 2) in this location, and b) that the SSS method can be used to predict the wind speed at the foremast anemometer locations with the same accuracy as the TM method.

3.3 Relative wind speed difference at the anemometer sites with severe flow distortion

Figure 4 and 5 compare the Y2002 in situ and CFD model estimates of the relative wind speed differences for the lifeboat deck and bridge vector anemometers with the SSS results. In both figures the wake of the foremast can be seen in the in situ data as a drop in the relative difference between relative wind directions of ±20° off the bow. The wake is far broader above the lifeboat deck than above the bridge since the former is caused by the foremast platform and legs of the frame, and the latter just by the mast that extends above the platform.

Figure 4 shows the results for the flow above the lifeboat deck. For four out of the five anemometers (A, B, C, E) the SSS results agree well with the in-situ data, with agreement of about 5 % or better, whereas the TM results disagree with the in-situ results by up to 17 %. In contrast, both the SSS and TM results for anemometer D overestimate the deceleration of the flow by 7 and 5 % respectively: the cause of this discrepancy is not known.

Figure 5 shows the results for the vector anemometers above the bridge, which as described above are a slightly better exposed than those located on the lifeboat deck. For all five Vector anemometers the agreement between the SSS model and the in situ data is excellent, with agreement to better than 2 % for the highest four anemometers and to 6 % for the lowest one (Vector E). The SSS results are significantly better than those found from the Y2002 TM model where the results differed from the in-situ data by between 8 and 14%.

It is noticeable from these results that the SSS simulation reproduced the mean flow in the wake regions remarkably well given that the models parameterise, rather than directly simulate, turbulence. Since both the SSS and the TM models solve the same equations and employ the same parameterisations, it is assumed that the greatly improved results from the SSS model are due to the large increase in mesh density: Table 2 shows that in the wake regions the cell sizes were halved, i.e. the mesh density increased by a factor of 8.

3.4 Absolute wind speed error and the vertical displacement

The absolute wind speed error (% difference from the undisturbed or free stream velocity) estimated from the SSS model was calculated for each anemometer site and is detailed with the Y2002 TM model estimates in Table 4. Wind speed errors identified as being closer to the in situ wind speed data in Sections 3.2 and 3.3 are indicated in bold type.

Both model estimates of the absolute wind speed error at the foremast anemometer locations and the main mast anemometer predicted a deceleration in the wind speed of about 1 % of the free stream flow. The general agreement between the model results at these anemometers is very good, with the results at all anemometer locations agreeing to within 0.2 %. The Solent sonic and the Young are located in symmetrically the same position on the foremast (Figure 2) and therefore the results for these two instruments should be the same. This symmetry is seen in the Y2002 results and is reproduced to within 0.1 % in the SSS results.

The wind speeds at anemometers in the regions of high flow distortion were decelerated by up to 20 % of the freestream flow. Where the differences between the two models was high (>3 %) the SSS model was generally in much better agreement with the in situ wind speed data, as discussed in Section 3.3.

In addition to being accelerated or decelerated, the flow of air over the ship may be displaced vertically due to the divergence of the airflow around the ship. Both model estimates of the vertical displacement of the airflow at all anemometer locations generally agreed to within 0.2 m.

4. Conclusions

Estimates of the wind speed error at anemometer sites on the RRS *Discovery* calculated using the VECTIS steady-state solver (SSS) have been validated against existing VECTIS model estimates which used the time marching (TM) solver and in situ wind speed data.

This study has shown that the results of the steady-state solver are equivalent to, or much better than, the Yelland et al. (2002) TM solver results. The SSS and TM results for the absolute wind speed at well-exposed anemometers agreed with each other to within 0.2 %, and both agreed with the in situ data to within 2 or 3 %. The agreement between model and in-situ results for anemometers located in regions of

severe flow distortion (above the bridge and lifeboat deck) were greatly improved when the SSS was used compared to the TM method. However, this is believed to be due to the increased cell resolution that can now be used, rather than the solver, as the same equations are solved in both models.

For numerical stability, the steady-state solver requires a much higher mesh density than the TM solver. In practice, a minimum of about 1 million cells are required for a research ship study using the SSS. This in turn requires about 1 Gb of memory and thus limits the use of the SSS to high-end PC's and workstations. However, for models with the same number of cells, using the steady-state solver reduces run times by about a factor of 7 compared to the TM method, e.g. a research ship modelled using 1 million cells can be modelled in 5 days using the SSS rather than a month or more using the TM solver.

If sufficient memory is available it is clear that using the steady state solver has the advantage of reducing model convergence times by a factor of seven compared to using the TM solver. If memory is limited to the point where the TM solver must be used then the impact of mesh density on the results must be considered, i.e. the mesh density in areas of low flow distortion may be adequate to ensure good results, but it is likely that the limitations imposed on mesh density in regions of severe flow distortion may result in a relatively poor simulation.

Acknowledgements

The research was funded by the National Oceanography Centre (UK) Technology Innovation Fund and the Woods Hole Oceanographic Institution.

References

Cowen, I. R., I. P. Castro, A. G. Robins, 1997: Numerical considerations for simulations of flow and dispersion around buildings*, Journal of Wind Engineering and Industrial Aerodynamics*, **67&68**, 525-545.

Ferziger, J. H., 2000: The physics and simulation of turbulence state of the art 1998, In J. P. A. J. Van Beek and C. Benocci (ed.), Introduction to the modelling of turbulence, *von Karman Institute for Fluid Dynamics lecture series*, von Karman Institute for Fluid Dynamics, Belgium, 39pp.

Launder, B. E. and D. B. Spalding, 1974: The numerical computation of turbulent flows, *Computer Methods in Applied Mechanics and Engineering*, **3**, 269-289.

Moat, B. I., 2003: Quantifying the effects of airflow distortion on anemometer wind speed measurements from merchant ships, *PhD. Thesis*, School of Engineering Sciences, University of Southampton, UK. 163 pp. [available from University of Southampton, UK., e-prints archive http://eprints.soton.ac.uk/]

Moat, B. I., M. J. Yelland, R. W. Pascal and A. F. Molland, 2005: An overview of the airflow distortion at anemometer sites on ships, *International Journal of Climatology (CLIMAR-II Special Issue),* **25**(7), 997-1006, DOI: 10.1002/joc.1177.

Moat, B. I., M. J. Yelland and E. B. Cooper, 2006: Airflow distortion at instrument sites on the RRS James Cook, *NOC Research and Consultancy Report No. 11*, National Oceanography Centre, Southampton. UK. 44pp. [available from University of Southampton, UK., e-prints archive http://eprints.soton.ac.uk/]

Ricardo, 2005: VECTIS user manual (Release 3.9), Ricardo Consulting Engineers Ltd, Shoreham-by –Sea, UK. [available from Ricardo Consulting Engineers Ltd, Bridge Works, Shoreham-by–Sea, West Sussex, BN43 5FG, UK]

Yelland, M. J., B. I. Moat, P. K. Taylor, R. W. Pascal, J. Hutchings and V. C. Cornell, 1998: Wind stress measurements from the open ocean corrected for air flow distortion by the ship, *Journal of Physical Oceanography,* **28**(7), 1511-1526.

Yelland, M. J., B. I. Moat, R. W. Pascal and D. I. Berry, 2002: CFD model estimates of the airflow over research ships and the impact on momentum flux measurements, *Journal of Atmospheric and Oceanic Technology*, **19**(10), 1477-1499.

Figures

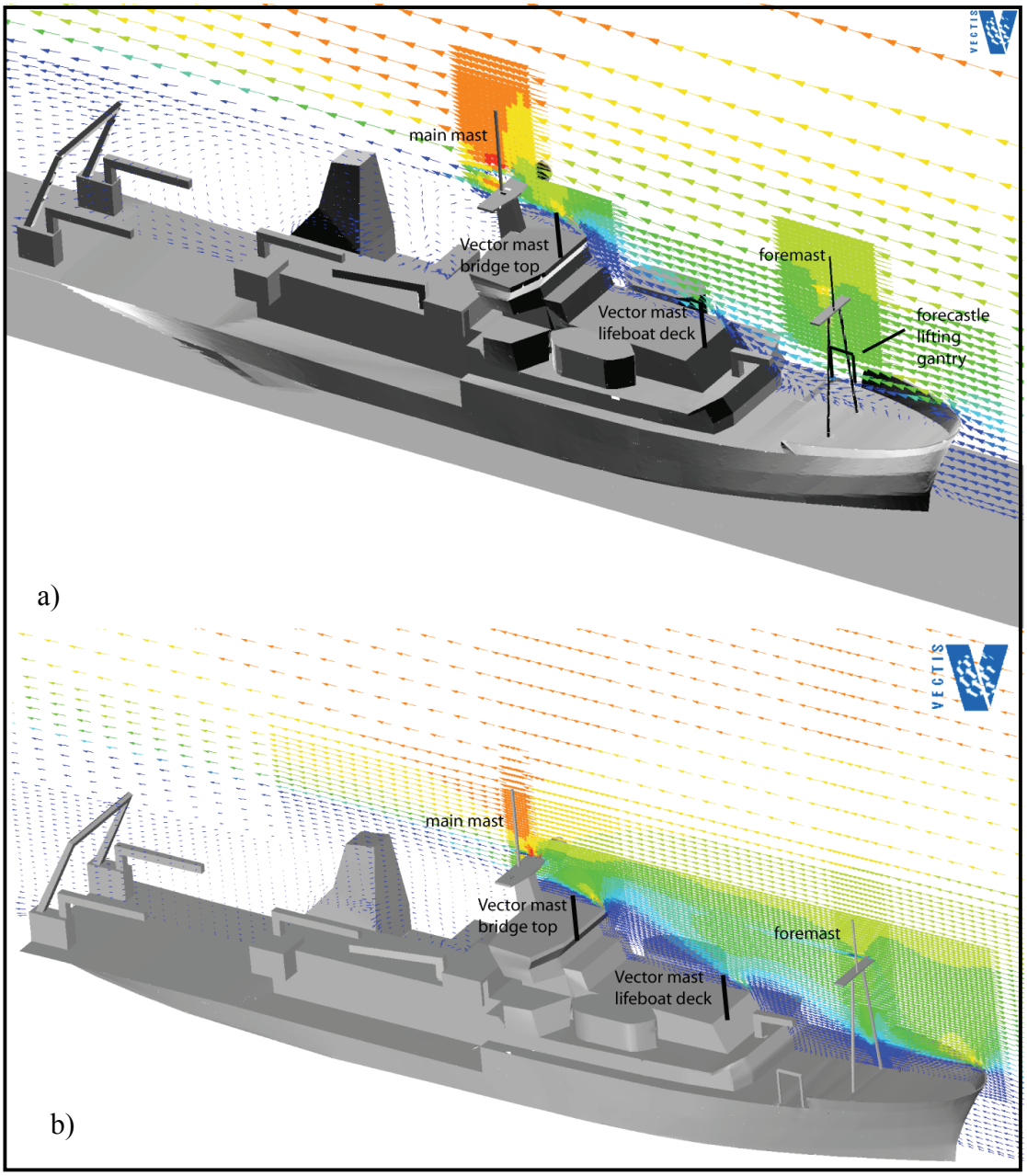

Figure 1 The CFD model simulations of the flow of air over the RRS *Discovery* using (a) the mesh of Yelland et al. (2002) and (b) that used in the current SSS simulation. The arrows represent the velocity of the flow in each computational cell, and the change in mesh density between the two simulations can be seen. Note that the geometries are identical except for the change in position of the forecastle lifting gantry.

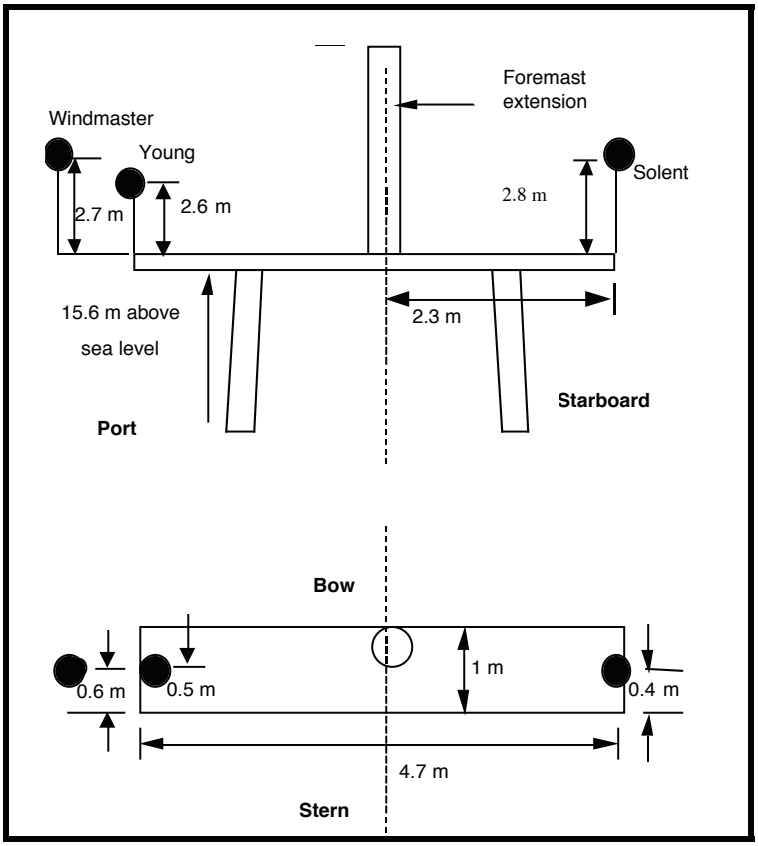

Figure 2 Positions of the foremast anemometers on the RRS *Discovery*, viewed from astern (top) and above (bottom). Reproduced from Yelland et al. (2002).

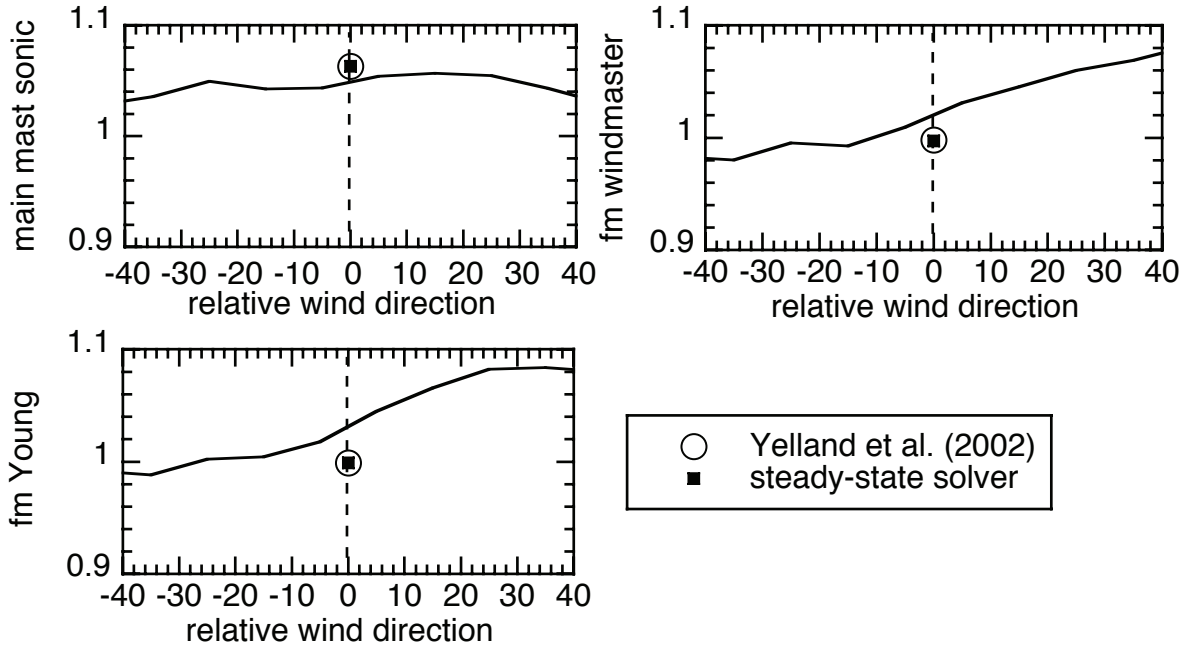

Figure 3 The relative wind speed differences (expressed as a fraction of the wind speed measured by the Solent sonic on the foremast on the foremast) from in situ wind speed measurements of Yelland et al. (2002) made on the RRS *Discovery* (lines) and from two CFD models (symbols). The standard errors ranged from 0.001 and 0.005 for the 10 degree averages of the in situ data. Relative differences are shown for (a) the Solent sonic on the main mast, (b) the Windmaster sonic on the foremast and (c) the Young on the foremast. The dotted lines indicate the bow-on flow (at 0°). Winds to port of the bow are shown by a negative wind direction.

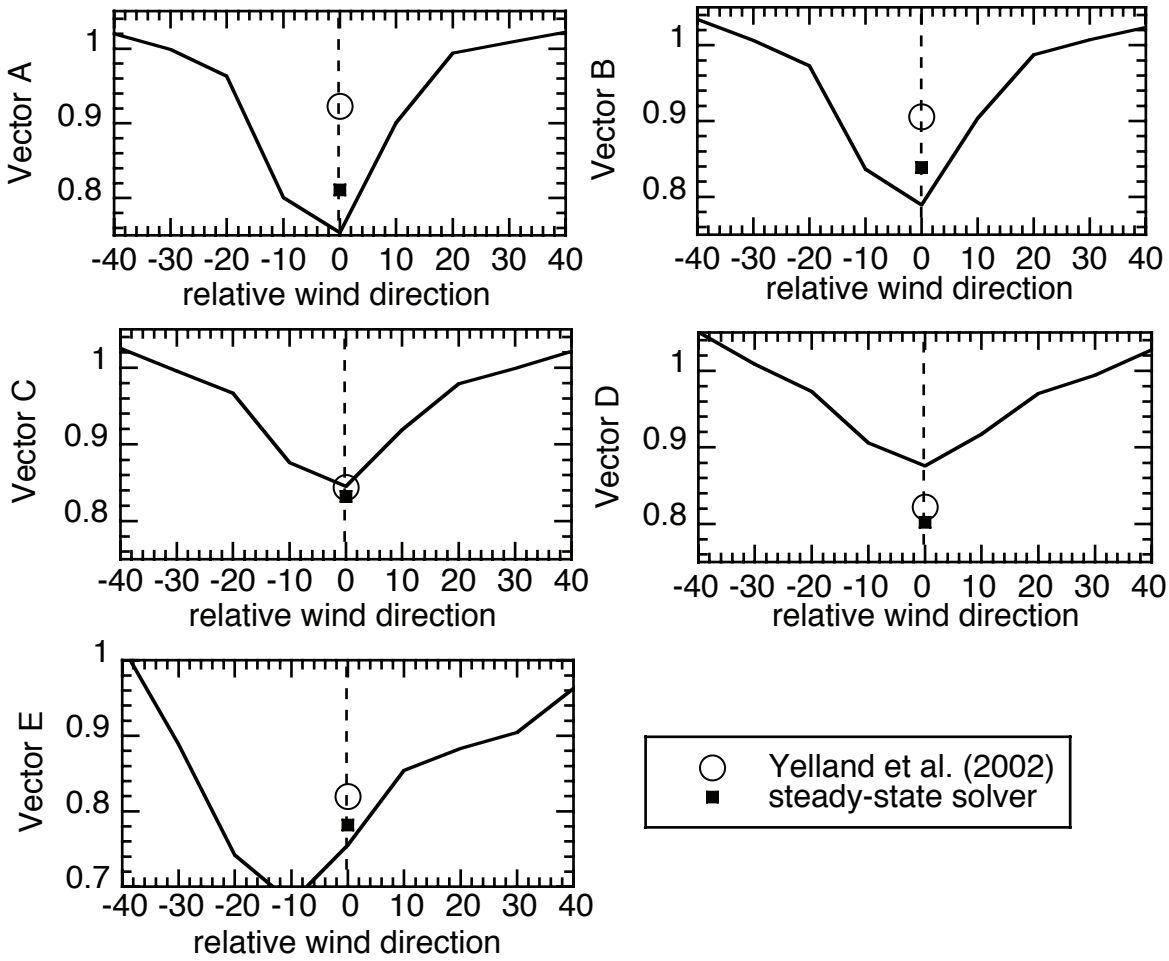

Figure 4 The relative wind speed differences (expressed as a fraction of the wind speed measured by the Solent sonic on the foremast on the foremast) from in situ wind speed measurements of Yelland et al. (2002) made on the RRS *Discovery* (lines) and from two CFD models (symbols) for the five vector anemometers located on the temporary mast on the lifeboat deck in front of the bridge. The vector anemometers are labelled A (highest) to E (lowest). The standard errors were typically between 0.002 and 0.007 for the 10° averages of the in situ data. The dotted lines indicate the bow-on flow (at 0°). Winds to port of the bow are shown by a negative wind direction.

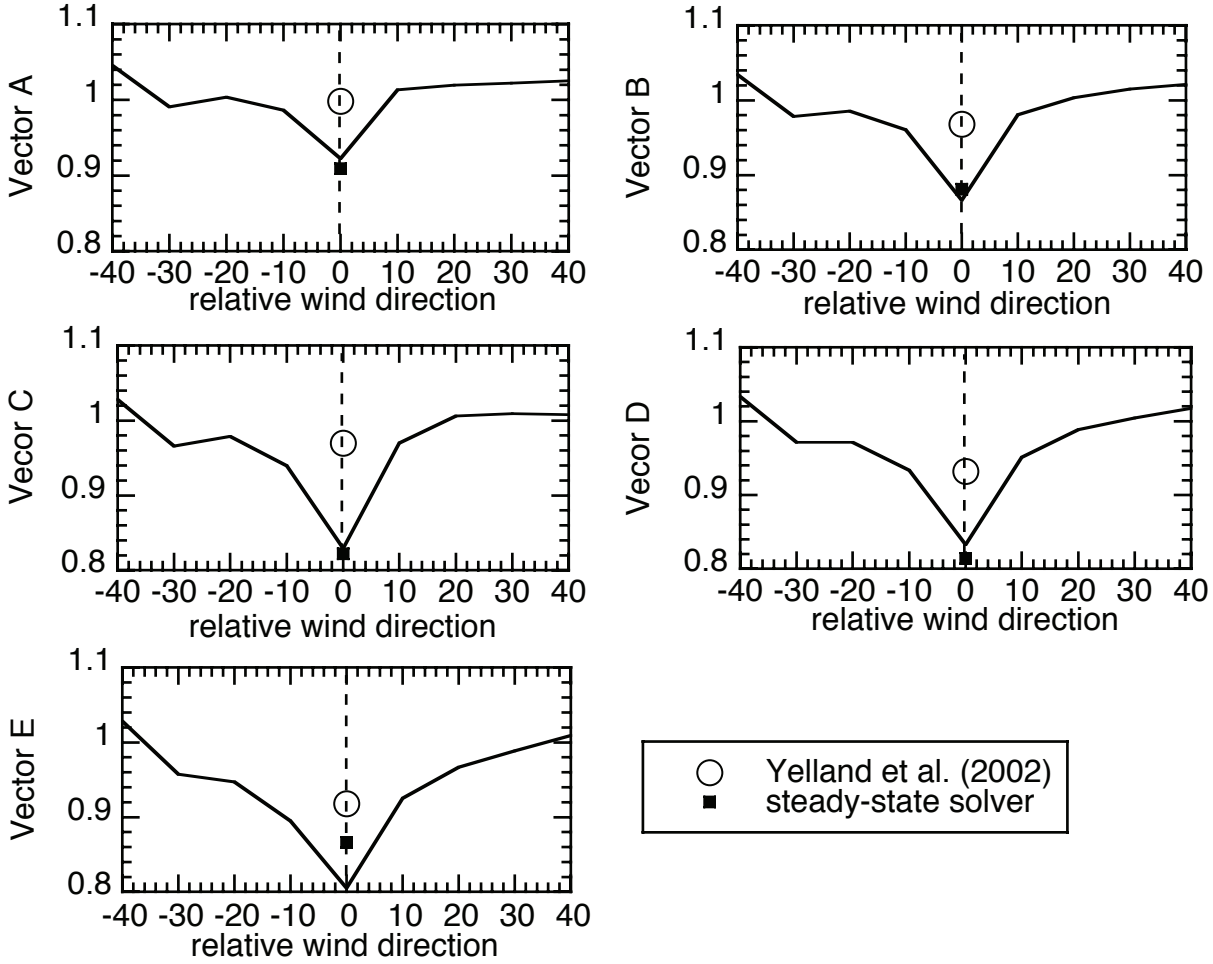

Figure 5 The relative wind speed differences (expressed as a fraction of the wind speed measured by the Solent sonic on the foremast on the foremast) from in situ wind speed measurements of Yelland et al. (2002) made on the RRS *Discovery* (lines) and from two CFD models (symbols) for the five vector anemometers located on the temporary mast on top of the bridge. The vector anemometers are labelled A (highest) to E (lowest). The standard errors were typically between 0.001 and 0.007 for the 10° averages of the in situ data. The dotted lines indicate the bow-on flow (at 0°). Winds to port of the bow are shown by a negative wind direction.

Tables

study	solver	No. of cells	run time	machine
recent simulations	TMS	500,000	3 weeks	LINUX 2.4 GHz Opteron processor
	TMS	1,000,000	6 weeks*	
present study	SSS	1,000,000	5 days	
Y2002	TMS	150,000	5 days*	
Y2002	TMS	150,000	3 weeks	SGI Indigo^2

Table 1 Run times for various VECTIS simulations. 'TMS' indicates the time marching solver and 'SSS' indicates the steady-state solver'. An '*' indicates an estimated time.

CFD simulation	Foremast site (m)	Lifeboat deck Vector anemometers (m)	Bridge Vector anemometers (m)	Main mast site (m)
Yelland et al. (2002)	0.6	1.2	0.6	1.6
steady-state solver	0.2	0.5	0.3	1.2

Table 2 Cell sizes at the anemometer locations in the two CFD simulations of the airflow over the RRS *Discovery*.

		height (m)	in situ	CFD simulations		difference (in situ – CFD)	
location	anemometer		Y2002	Y2002	SSS	Y2002	SSS
foremast	Windmaster	18.58	1.02	**0.998**	0.997	0.022	0.023
	Young	18.46	1.03	0.999	0.999	0.031	0.031
main mast	Solent Sonic	18.36	1.04	**1.06**	1.063	-0.020	-0.023
mast on life-boat deck	Vector A	25.20	0.754	0.923	**0.811**	-0.169	-0.057
	Vector B	15.94	0.790	0.906	**0.839**	-0.116	-0.049
	Vector C	14.94	0.845	**0.844**	0.832	0.001	0.013
	Vector D	13.94	0.876	**0.822**	0.802	0.054	0.074
	Vector E	12.94	0.755	0.820	**0.782**	-0.065	-0.027
mast on top of bridge	Vector A	11.94	0.922	0.998	**0.909**	-0.076	0.013
	Vector B	20.15	0.866	0.968	**0.881**	-0.102	-0.015
	Vector C	19.15	0.829	0.970	**0.822**	-0.141	0.007
	Vector D	18.15	0.833	0.932	**0.814**	-0.099	0.019
	Vector E	17.15	0.805	0.918	**0.866**	-0.113	-0.061

Table 3 Difference between the CFD estimates and the in situ relative differences (speed at anemometer site / speed at site of Solent sonic on foremast) as shown in Figures 2 to 4. The bold type indicates the model that is in better agreement with the in situ data.

Location	Anemometer	Absolute wind speed error at z_{anemom} (%)		Difference (%)	Absolute wind speed error at $z_{anemom} - \Delta z$ (%)		difference	Vertical displacement (m)		difference
		Y2002	SSS		Y2002	SSS		Y2002	SSS	
foremast	Solent Sonic	**-0.8**	-0.7	0.1	**-0.4**	-0.2	0.2	1.1	1.1	0.0
	Windmaster	-1.0	-0.9	0.1	-0.6	-0.4	0.2	1.1	1.1	0.0
	Young	-0.8	-0.6	0.2	-0.4	-0.2	0.2	1.0	1.2	0.2
main mast	Solent Sonic	3.0	3.1	0.1	3.8	3.8	0.0	2.3	2.3	0.0
mast on life-boat deck	Vector A	-7.5	**-18.5**	11	-6.9	**-17.9**	11.0	1.6	1.4	0.2
	Vector B	-8.8	**-15.3**	6.5	-8.1	**-14.5**	7.3	1.6	1.6	0.0
	Vector C	**-14.7**	-15.5	0.8	**-14.0**	-14.8	0.8	1.6	1.5	0.0
	Vector D	**-16.5**	-18.1	1.6	**-15.8**	-17.2	1.4	1.5	1.7	0.2
	Vector E	-16.1	**-19.7**	3.6	-15.6	**-18.9**	3.3	1.4	1.5	0.1
mast on top of bridge	Vector A	-1.6	**-10.2**	8.6	-0.7	**-9.1**	8.4	2.5	2.9	0.4
	Vector B	-4.3	**-12.6**	8.3	-3.3	**-11.4**	8.1	2.8	3.0	0.2
	Vector C	-3.7	**-18.2**	14.5	-2.7	**-17.0**	14.3	2.8	3.1	0.3
	Vector D	-7.1	**-18.6**	11.5	-6.1	**-17.4**	11.3	2.7	2.9	0.2
	Vector E	-8.2	**-12.8**	4.6	-6.9	**-11.4**	4.5	3.1	3.1	0.0

Table 4 The type, location and height above sea level of the anemometers. The absolute wind speed error is expressed as a percentage of the freestream speed at the actual anemometer height (z_{anemom}) and the effective anemometer height ($z_{anemom}-\Delta z$). CFD model estimates of the vertical displacement of the flow (Δz) are given for each site. The bold type indicates the model that is in better agreement with the in situ data, as determined from the relative differences in Table 3.